Microwave Properties of Rock Salt and Lime Stone for Detection of Ultra-High Energy Neutrinos

Toshio Kamijo*[a] and Masami Chiba*[b]
[a]Graduate School of Engineering; [b]Graduate School of Science
Tokyo Metropolitan University, Tokyo Japan

ABSTRACT

Rock salt and lime stone are studied to determine their suitability for use as a radio wave transmission medium in an ultra high energy (UHE) cosmic neutrino detector. Sensible radio-wave would be emitted the Askar'yan effect (coherent Cherenkov radiation from negative excess charges in an electromagnetic shower) in the interaction of the UHE neutrinos with the high-density medium. If the attenuation length in the material is large, relatively small number of radio-wave detector could detect the interactions happened in the massive material. We have been measured the complex permittivity of the rock salts and lime stones by a free space method and a perturbational resonator method at 9.4GHz. In this paper, we show the data for new lime stone samples from Mt. Jura in France at 9.4GHz and the results of preliminarily measurements of the frequency dependency at 7-12GHz. The measured value of the radio-wave attenuation lengths of the rock salt sample from the Hockley salt mine in USA is longer than 4.7m at 9.4 GHz and then under the assumption of constant $\tan\delta$ with respect to frequency, we estimate it by extrapolation to be longer than 440 m at 100 MHz. The results show that there is a possibility to utilize natural massive deposits such as rock salt for a UHE neutrino detector.

Keywords: Ultra-high energy neutrino, Attenuation length, Coherent-Cherenkov effect, Complex permittivity, Rock salt, Lime stone

1. INTRODUCTION

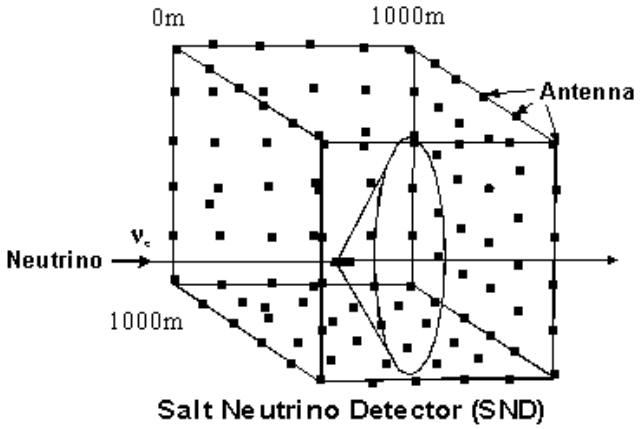

Figure 1: Underground Salt Neutrino Detector. Excess electrons in the shower from the UHE neutrino interaction generate coherent Cherenkov radiation with an emission angle of 66°.

Several cosmologically distant astrophysical systems, e.g. active galactic nuclei, produce ultra-high-energy (UHE) cosmic neutrinos[1] of energies over 10^{15} eV (PeV). Though the flux is very low, probably it exceeds that of atmospheric neutrinos[2]. Therefore, despite the low flux and the low cross section[3], we can identify extraterrestrial neutrinos coming from distances over 50 Mpc (163 million light years) without the Greisen, Zatsepin and Kuz'min (GZK) cutoff[4] and an atmospheric neutrino background. In spite of the GZK cutoff, mysteriously protons of energies over 10^{20}eV arrive to the earth[5]. On the other hand, neutrinos do not effected by GZK cutoff, they could travel longer distance than protons.

The aim of UHE-neutrino detection is to study (1) the UHE neutrino interaction, which is not afforded by artificial neutrino beams generated in an accelerator[6], (2) the neutrino mass problem through the neutrino oscillation effect after a long flight distance[7] and (3) the UHE accelerating mechanism of the protons existing in the universe.

*contact [a] kamijo@eei.metro-u.ac.jp; [b] chiba-masami@c.metro-u.ac.jp; 1-1 Minami-ohsawa, Hachiohji-shi, Tokyo, Japan.

In order to detect UHE neutrinos, we need a detector with a huge mass (at least 10^9 tons) since neutrinos interact in the detector volume only via weak interactions and the flux of UHE neutrinos is very low. However, from a practical point of view, it is difficult to construct such a huge detector. We are therefore interested in the possibility of using a natural rock salt mine as a UHE neutrino detector, a Salt Neutrino Detector (SND)[8]. Rock salt deposits are distributed world wide so there are many candidates for suitable sites[9]. Rock salt deposit does not allow water penetration, which hinders radio wave transmission. Fig.1 shows a scheme for an SND using a large volume (1km×1km× 1km) of salt dome.
In order to measure UHE neutrinos effectively, the mass of a detector should be considerably greater than that of the existing large neutrino detector, the Super Kamiokande (S-K), Kamioka, Gifu, Japan, which consists of 5×10^4 tons of pure water[10]. The S-K detects visible light generated by the Cherenkov Effect in pure water. The transparency (attenuation length) of pure water is 100 m at most.
Rock salt, on the other hand, is one of the most transparent materials for radio waves[8, 11-13] as well as ice[14]. Therefore a moderate number of radio wave sensors could detect neutrino interactions in the massive rock salt. G. A. Askar'yan has proposed detecting radio emissions with coherent amplification produced by excess negative charges of electron-photon showers in dense materials, the Askar'yan Effect[15], which could be used to detect the interaction of UHE neutrinos with high-density media. While for the radio wave emission from the air shower, a thin material, the same effect was calculated independently by M. Fujii and J. Nishimura[16]. Recently the Askar'yan Effect was confirmed by a bunched electron beam in an accelerator[17]. The transparency to electromagnetic waves in the microwave region or longer wavelengths is expected to be large in rock salt. Therefore a moderate number of radio wave sensors could detect neutrino interactions in the massive rock salt[12, 20].
Unfortunately, no natural rock salt deposits are located in Japan. At the age of rock salt formation, Japan was under the sea, and hence there was no possibility for deposits to form. To find possible locations for constructing an SND we have visited five rock salt mines outside Japan and taken samples of the rock salt. We have also considered the possibility of using lime stone as a detector mass. In Japan lime stone mines are abundant and the proportion of $CaCO_3$ in Japanese lime stone is over 95%, compared with around 80% in lime stone from overseas sources. We have taken samples of lime stone from a mine at Kamaishi, Japan and Mt. Jura, France to examine its viability as a detector.
We have previously reported measurements of the complex permittivities of rock salt samples by a free space method[18]. In the present report we present results of measurements of rock salt and lime stone samples by a perturbation method using cavity resonator in which the precision of the imaginary part (the attenuation in a medium) of the permittivities is improved.

2. CONSIDERATION ON THE MEDIUM FOR CHERENKOV EFFECT

We compare density, radiation length, refractive index, Cherenkov angle and threshold kinetic energy of electrons for air, ice, rock salt and lime stone in Table 1.

Media	Density(g/cm^3)	X_0 (cm)	Refractive Index n	θ_c (deg)	T_{th} (keV)
Air (STP)	0.0012	30420	1.000293	1.387	2060407
Ice (H_2O)	0.924	39	1.78	55.8	107
Rock salt (NaCl)	2.22	10.1	2.43	65.7	50
Lime stone ($CaCO_3$)	2.7	9.0	2.9	69.8	33

Table 1: Comparison among air, ice, rock salt and lime stone in density, radiation length X_0, refractive index n, Cherenkov angle θ_c and threshold kinetic energy for electrons T_{th}.

The density of air is 1/833 times less than rock salt and the radiation length is 3042 times larger than that even on the earth surface. Then the shower length and the diameter are much larger than ice, rock salt and lime stone. The detection is not easy for such a horizontal extended air shower produced by neutrinos. In addition Cherenkov or fluorescent light detection in air shower depend on weather condition severely as well as the Sunlight, the Moonlight, lightning and artificial light. Underground detectors neither depend on the weather nor the Sunlight and the Moonlight. In principle they could furnish the same detection ability for all the time and the directions of the neutrino incidence.
In comparison with ice, rock salt has 2.4 times higher density, shorter radiation length (~1/4) and 1.4 times larger refractive index. Further lime stone has 20% larger density and 10% shorter radiation length than rock salt. Then the high-energy particle shower size is small. For electrons, the Cherenkov angle is large and the threshold energy is small due to the high refractive index. Consequently, rock salt is adequate medium to get larger Cherenkov radiation power.

The frequency at the maximum electric field strength at θ_c is ~2 GHz without the absorption in ice[14]. Whereas it would increase up to ~5.6 GHz taking into account the short radiation length and the wavelength contraction due to the higher refractive index. For lime stone 20% larger refractive index yields larger Cherenkov angle and the lower threshold electron energy as low as 33 keV.
When a UHE proton hits the atmosphere, it could not put the large energy deposit underground in a narrow region. Radio-wave neutrino detector could sense only from many tracks of excess electrons inside the concentrated region with the help of strengthening by the coherence effect. For high sensitivity detector e.g. optical Cherenkov detectors, which could detect single muons, a great number of downward muons become large backgrounds. On the contrary the radio Cherenkov detector senses detect a UHE muon (>10^{15} eV) only when it deposits large energy (>10^{15} eV) in a small region, by a deep inelastic scattering. The muon could be generated at the proton-atmosphere interaction directly. At this moment, the probability is estimated to be lower than the neutrino interaction. Therefore, practically only UHE neutrinos could induce the electric field on the radio antennas underground. However it could be a shortcoming when we intend to detect abundant lower-energy neutrinos in high statistics.
Normally, rock salt is covered by thick soil, which absorbs electromagnetic wave completely. Then SND is background free from natural or artificial radio wave coming from the surface on the earth. As a result background is only blackbody radiation corresponding to the temperature of the surrounding rocks. As the remaining potential background, radiation may come from a seismic movement of the surrounding rocks, which may generate radio wave due to the piezoelectric effect by the stress in the rocks. If such a radiation could be detected, the observation contributes to the seismology.

3. MEASUREMENT OF COMPLEX PERMITTIVITY USING METAL-BACKED SHEET SAMPLES BY THE FREE SPACE MEASUREMENT METHOD.

We restate briefly our results of the free space measurement method on rock salt[8]. Three rock salt samples were used for the measurement of the complex permittivity by the free space measurement method. Two were taken from the Hallstadt salt mine in Austria and the third from the Asse salt mine in Germany. Each of the samples was prepared into flat sheets 200mm×200mm square. The reflection coefficients of the metal-backed sheet samples were measured without the influence of extraneous scattering waves.
A free space measurement method was employed and is illustrated in Fig. 2. This method has been used in a non-destructive manner for the assessment of microwave absorbers[18]. An important feature of this method is the ability to get rid of the various extraneous waves from the signal of the received antenna. Components of the extraneous waves are direct wave between the transmitting antenna and the receiving antenna, scattering from the walls, ceiling, floor, support, parts of the sample outside the measuring area and so on. The scattering of interest is that of the area where the metal-plate reflector is placed, namely the measuring area. The method involves measuring the amplitude and phase of scattered radiation with and without a metal-plate reflector on the sample. We use a vector network analyzer HP85107A System to make the vector measurements. By making measurements of the scattered radiation first with and then without the metal-plate reflector, the incident radiation and the radiation scattered off the measuring area can be separated from the extraneous waves. The behavior of the metal-plate reflector is similar to that of an optical shutter in optics.
In Fig. 2, the illustration shows three metal plates piled up on the sample to keep the reflector surface elevated. The receiving antenna may be set up for either measuring reflected or transmitted radiation. In practical samples, only the reflection coefficient is measured. We consider here the reflective case. $\boldsymbol{E_m}$ and $\boldsymbol{E_s}$ refer to reflected signals from the metal plate and the sample at the measuring area, respectively. $\boldsymbol{E_d}$ refers to total extraneous waves mentioned above. The received signals $\boldsymbol{E_{rm}}$ and $\boldsymbol{E_{rs}}$ are the reflected signals from the metal-plate reflector $\boldsymbol{E_m}$ with the background signal $\boldsymbol{E_d}$, and from the measuring area of the sample $\boldsymbol{E_s}$ with the background signal $\boldsymbol{E_d}$, respectively. The height of the metal-plate reflector is raised to give a small difference in the path length between the antennas and the metal-plate reflector, which alters the phase of the reflected wave from the metal-plate reflector only. In the vector diagram, the horizontal and the vertical axes express the real and the imaginary coordinates. The large and small circles show the cases with and without the metal-plate reflector. Different heights of the metal-plate result reflector in different path lengths, expressed as h = 0, h_1, h_2 and h_3 on the large circle and the $\boldsymbol{E_m}$ vectors are shown (note that the receive signal $\boldsymbol{E_{rm}}$ is illustrated only for the case of h = 0). On the small circle, $\boldsymbol{E_s}$ is shown only at h = 0, without the metal-plate reflector. The center of each of the circles defines $\boldsymbol{E_d}$, and hence it can be deducted vectorically and the background

extraneous waves eliminated. The complex permittivity can be deduced from the reflection coefficients, the ratio of the complex reflection coefficients, $\boldsymbol{R_{p,s}} = \boldsymbol{E_s} / \boldsymbol{E_m}$, where p and s refer to parallel and perpendicular polarizations with respect to the scattering plane.

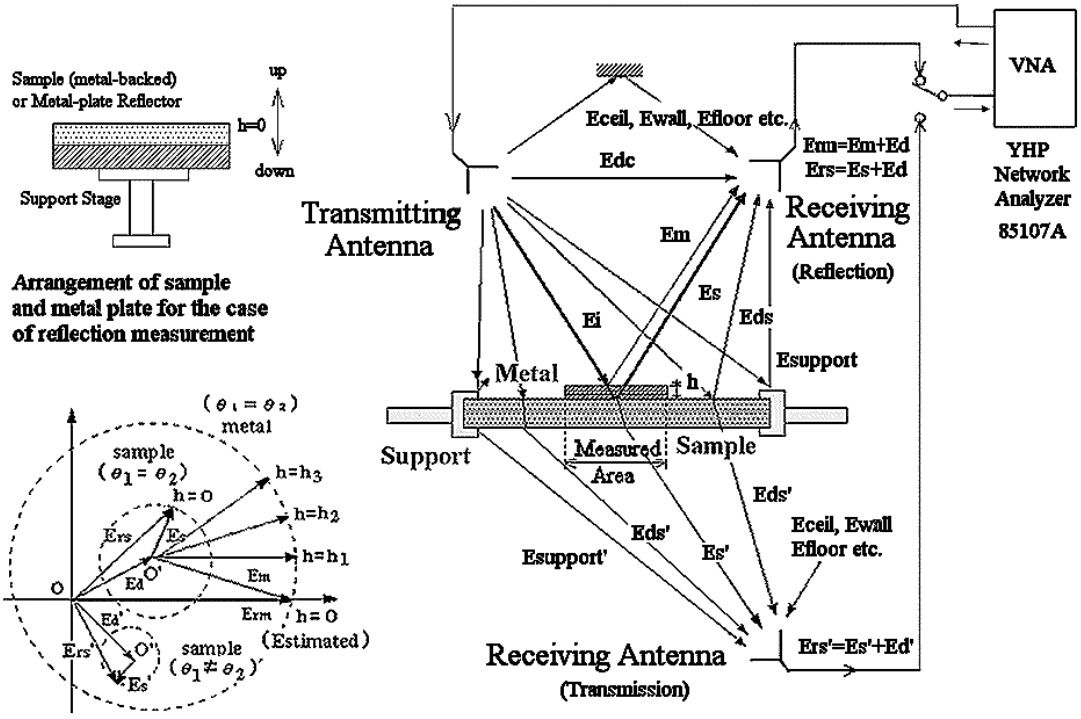

Figure 2: The principle of the measurement of the free space method showing the various wave components. The signals both with and without the metal-plate reflector on the sample are also shown in a vector diagram[18].

The calculated real part of the complex permittivities of the three samples derived from $\boldsymbol{R_p}$ and $\boldsymbol{R_s}$ are tabulated in Table 2. The estimated uncertainty in each of the real values is ± 0.2. The values of the real part are consistent each other and with the value of 5.9 in the reference material[11].

Sample thickness	Calculated from R_p	Calculated from R_s
(a) Hallstadt 11.1mm	5.9 ± 0.2	6.0 ± 0.2
(b) Hallstadt 30.1mm	5.9 ± 0.2	6.0 ± 0.2
(c) Asse Mine 99.0mm	5.9 ± 0.2	5.9 ± 0.2

Table2: Real part of complex permittivities in rock salts at 9.4GHz.

We can calculate the attenuation coefficient α for the case of a low loss material from the equation

$$\alpha = \frac{\omega}{c}\sqrt{\varepsilon'}\,\frac{\tan\delta}{2}, \tag{1}$$

where the complex permittivity ε is

$$\varepsilon = \varepsilon' - j\varepsilon'' = \varepsilon'(1 - j\tan\delta), \tag{2}$$

and the loss angle in the permittivity $\tan\delta$ is

$$\tan\delta = \frac{\varepsilon''}{\varepsilon'}. \tag{3}$$

From ε and $\tan\delta$ we can calculate the complex refractive index n,

$$n = \sqrt{\varepsilon} = \sqrt{\varepsilon'}\sqrt{1 - j\tan\delta}. \tag{4}$$

After traveling a distance z through a material, the complex electric field of the electromagnetic wave $\boldsymbol{E_0}$ becomes $\boldsymbol{E}$,

$$E = E_0 e^{j\omega t - (\alpha + j\beta)z} = E_0 e^{-\alpha z} e^{j(\omega t - \beta z)} \tag{5}$$

where the propagation constant $\boldsymbol{\gamma} = \alpha + \boldsymbol{j}\,\beta$ can be expressed as

$$\alpha + j\beta = j\omega\sqrt{\varepsilon_o \mu_0}\,\sqrt{\varepsilon' - j\varepsilon''}. \tag{6}$$

The scalar electric field decreases as

$$|E| = |E_0| e^{-\alpha z} \tag{7}$$

Therefore the electric field attenuation length L_α where the field strength decreases by a factor of 1/e is

$$L_\alpha = \frac{1}{\alpha} = \frac{c}{\pi f \sqrt{\varepsilon'}\tan\delta} \tag{8}$$

The measurement accuracy was insufficient to allow the imaginary part of the permittivity to be calculated. We found that the imaginary permittivity had different values for samples (a) and (b), even though both were cut from the same block. We were able to estimate that the imaginary part of the permittivity is less than 0.1, or $\tan\delta$ is less than 0.017 at 9.4 GHz. Using our estimate for the upper limit of $\tan\delta$ of 0.017, we calculate a lower limit on α of 4.1 m^{-1} at 9.4 GHz. Hence the attenuation length L_α is greater than 0.24 m at 9.4 GHz. Assuming that $\tan\delta$ is constant with respect to frequency; the attenuation length is larger than 24 m at 94 MHz.

Unfortunately, the accuracy of this method as used in this experiment is too poor for these low $\tan\delta$ samples. A more accurate value for $\tan\delta$ could be achieved if we used a sample with a larger area and thickness and used the transmission configuration. This method also has the advantage in that it can be modified to make *in situ* measurements. However, in order to improve our results we have chosen to measure the permittivities of rock salt and lime stone using the cavity perturbation method.

4. MEASUREMENT OF COMPLEX PERMITTIVITY USING A SMALL STICK SAMPLE BY THE CAVITY PERTURBATION METHOD.

We have measured natural rock salt samples by the perturbed cavity resonator method[19] at 9.4GHz. The measuring system is shown in Fig. 3. A drawing and photograph of the rectangular cavity are shown in Fig. 4. Note that there are no sample insertion holes in the cavity with sample insertion device. For this perturbation method, small samples, such as 1mm×1mm×10.2mm, should be used in order to avoid changing the resonance behavior significantly, e.g. inducing only a small shift in the resonance frequency and resonance width. In addition, the electric field strength should be uniform over a cross section of the sample. It is difficult to cut fragile samples to this size. Mechanical cutting using a milling machine was unsatisfactory for our natural rock salt samples. Synthesized rock salt in single crystals could be cleaved to the size, but it was difficult to cleave natural rock salt and slightly thicker samples of natural rock salt had to be used. Lime stone is strong enough and we could cut it with a milling machine.

Magnetic field couplings were used for the input and output couplings. The cavity width (in the x-direction) and height (in the y-direction) were set to a = 22.9 mm and b = 10.2 mm (the size of waveguide for X-band), respectively. The cavity length L (in the z-direction), however, was adjustable so that filling factor F of the sample could be varied. The resonance mode is defined by the parameter $TE_{10n,}$ where the three numbers of the subscript refer to the number of nodes in the x, y and z directions respectively, i.e. there is 1 node in the x direction, 0 in the y direction and n for the z direction can be varied by varying the length of the cavity. With the sample in the center of the cavity, n can be set to 1, 3, 5, 7 or 9, and refers to the number of half guided-wavelengths $\lambda_g/2$ in the wave-guide. Hence n is set by varying the length of the cavity with each half wavelength equal to $\lambda_g/2$ = 22.2 mm.

For these measurements, we take n = 7 to give a sharp resonance in the cavity at 9.4GHz. This gives a cavity resonator length of L = 155.4 mm. The resonance wavelength λ_0 is calculated by

$$[\frac{1}{\lambda_0}]^2 = [\frac{1}{2a}]^2 + [\frac{n}{2L}]^2. \quad (9)$$

For the values of n, L and a defined above the free space wavelength λ_0 becomes 31.9 mm with a frequency of c/λ_0 = 9.4 GHz.

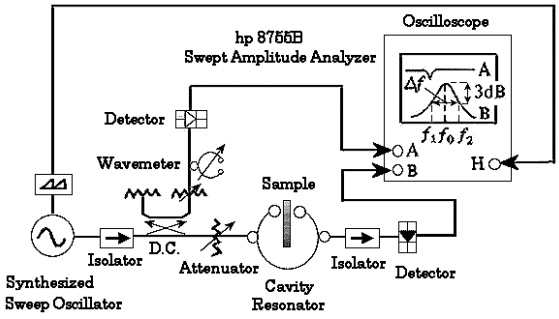

Figure 3: Drawing of the cavity resonator system.

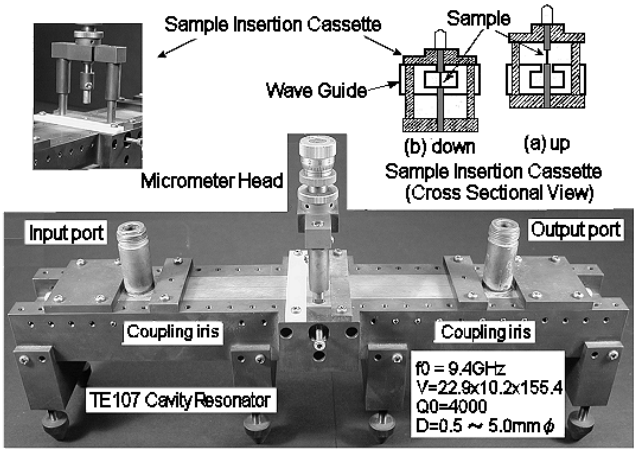

Figure 4: Illustration and photograph of the perturbed cavity resonator without insertion holes[19].

Using this apparatus the complex permittivity $\boldsymbol{\varepsilon}$ could be measured. The principle of the measurement is to derive the real and imaginary parts of the complex permittivity, ε' and ε'', from the changes in the center frequency and the width of the resonance, respectively. Measurements were made both with and without the insertion of the sample in the cavity. The real ε' is found from the change in resonance frequency when the sample is placed in the cavity,

$$\frac{-(f - f_0)}{f_0} = \alpha_\varepsilon(\varepsilon' - 1)\frac{dV}{V} \quad (10)$$

where f and f_0 are the resonance frequencies with and without the sample in the cavity, dV and V are the volumes of the sample and the cavity resonator, and α_ε is a constant determined by the mode of the cavity and the sample position relative to the electric field maximum; equal to 2 in this case of TE_{107}. Note that the appearance of dV/V indicates that the size of the sample impacts on the perturbation of the resonance behavior and hence a small stick-shaped sample should be used.

The imaginary ε'' depends on the change in the Q factor,

$$\frac{1}{2}[(\frac{1}{Q}) - (\frac{1}{Q_0})] = \alpha_\varepsilon \varepsilon'' \frac{dV}{V} \quad (11)$$

where Q and Q_0 are f/df and f_0/df_0, respectively, and df (~2.7MHz) and df_0 (~2.5MHz) are the resonance widths measured at a height of -3dB below the peak height. The inverse Q difference $(1/Q - 1/Q_0)$ is defined as $1/Q_s$. Equations (10) and (11) is called perturbation formula. The measured Q_0 was found to be around 4000. A radio frequency signal was supplied to the cavity resonator by a synthesized CW generator (Anritsu 68047C) and Q was measured by a HP8755B swept amplitude analyzer. Recently, the measurements are conducted by HP 85107A Network Analyzer system. The absolute uncertainty of the frequency measurements was well under 1×10^{-5}.

The measurement uncertainty in ε' comes from an uncertainty of ~10 kHz from measuring the resonance peak frequencies and an uncertainty of ~0.001 mm^3 from measuring the volumes of the cavity and the sample. The largest contribution to the uncertainty in determining ε' was from the measurement of dV. The sample volume was measured by a microscope furnished with movable x-y micrometers. We estimate an uncertainty in ε' of 3%.

The uncertainty in ε'' is mainly due to the uncertainty in measuring the resonance width, ~100 kHz, with and without the sample. After the calculation, the estimated uncertainty in ε'' is 2.5×10^{-4}. The variation in the measured values is greater

than this uncertainty, even though those samples were cut from the same block. This variation may be due to differences in impurity through the block and hence the ε'' of a sample depends on where the sample is cut from the block. Differences in the smoothness of the surface, the stain and the moisture content may also lead to variations in ε''. In addition, the apparatus itself may lead to variations. Multiple reflections of the radio wave in the input and output wave guides between the cavity and the RF generator and between the cavity and the detector might lead to changes in the output amplitude. We decreased these errors by inserting the isolators in front of the cavity and the backward of the cavity.

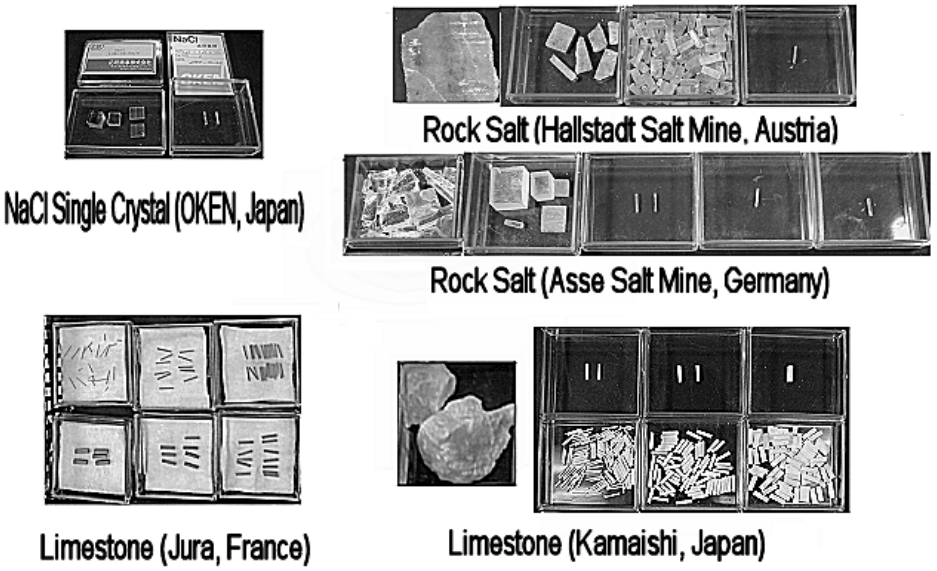

Figure 5: Samples measured with the perturbative cavity resonator.

Sample	ε'	$\varepsilon'' \times 10^{-3}$	$\tan\delta \times 10^{-4}$	α at 9.4GHz (m^{-1})	$L_\alpha = 1/\alpha$ at 9.4GHz (m)
Single crystal (NaCl)	5.8 ± 0.2	3.2 ± 0.3	5.5 ± 0.5	0.13 ± .01	7.7±0.7
Rock Salt, Asse, Germany	5.8 ± 0.2	<7.8	<13	<0.31	>3.3
Rock Salt, Hallstadt, Austria	5.8 ± 0.2	<44	<76	<1.8	>0.56
Rock Salt, Hockley, USA	5.9 ± 0.2	5.5	9.0	0.21	4.7
Lime stone ($CaCO_3$) Kamaishi, Japan	9.0 ± 0.2	20	22	0.54	1.9
Lime stone ($CaCO_3$) Mt. Jura, France	8.7 ± 0.2	60	69	1.7	0.59

Table 3: Comparison among single crystal NaCl, Asse rock salt, Hallstadt rock salt, Hockley rock salt, Kamaishi lime stone and Jura lime stone in ε', ε'', $\tan\delta = \varepsilon''/\varepsilon'$, α at 9.4GHz, $1/\alpha$ at 9.4GHz.

Sample	Cross section (mm)	*dV/V*	Linearity of $-(f - f_0)/f_0$ in *dV/V*	Linearity of $1/Q_s$ in *dV/V*
Single crystal (NaCl)	1.0×1.1 – 1.0×1.6	3.2×10^{-4}–4.6×10^{-4}	-	-
Rock Salt, Asse	1.7×1.8 – 3.0×3.1	8.5×10^{-4}–2.7×10^{-3}	1.7×10^{-3}	?
Rock Salt, Hallstadt	2.1×1.8 – 3.0×3.0	1.0×10^{-3}–2.5×10^{-3}	2.5×10^{-3}	?
Rock Salt, Hockley	1.2×1.2 – 1.5×1.6	3.5×10^{-4}–6.7×10^{-4}	0.7×10^{-3}	0.5×10^{-3}
Lime stone ($CaCO_3$) Kamaishi, Japan	1.0×1.0 – 3.0×2.9	2.7×10^{-4}–2.4×10^{-3}	1.1×10^{-3}	1.1×10^{-3}
Lime stone ($CaCO_3$) Jura, France	0.5×0.4 – 3.0×3.1	5.7×10^{-5}–2.6×10^{-3}	1.1×10^{-3}	1.1×10^{-3}

Table 4: Comparison among single crystal NaCl, Asse rock salt, Hallstadt rock salt, Hockley rock salt, Kamaishi lime stone and Jura lime stone in sample cross section, *dV/V*, linearity of $-(f - f_0)/f_0$ and $1/Q_s = 1/Q - 1/Q_0$ in *dV/V*

We were able to cleave four synthetic rock salt samples into single crystals of cross sections ranging from 1.0mm×1.1mm to 1.0×1.6mm with filling factors dV/V of 3.2×10^{-4} to 4.6×10^{-4}. For filling factors this small ε' and ε'' are not affected by perturbations to the resonance due to the presence of the sample. For synthetic rock salt, we found an average $\varepsilon = (5.8 \pm 0.2) - j\,(3.2 \pm 0.3)\times 10^{-3}$ or $\tan\delta = (5.5 \pm 0.5)\times 10^{-4}$, which is consistent with the values given in Ref. 11. We have succeeded in cleaving samples of natural rock salt from the Asse salt mine in Germany, the Hallstadt salt mine in Austria and the Hockley salt mine in USA, and also milled samples of lime stone from the Kamaishi lime stone mine in Japan and Mt. Jura in France. The samples were formed into small sticks of length 10.2 mm, equal to the height of the cavity resonator. Fig. 5 shows a photograph of these small stick samples and their cross sections are listed in Table 3.

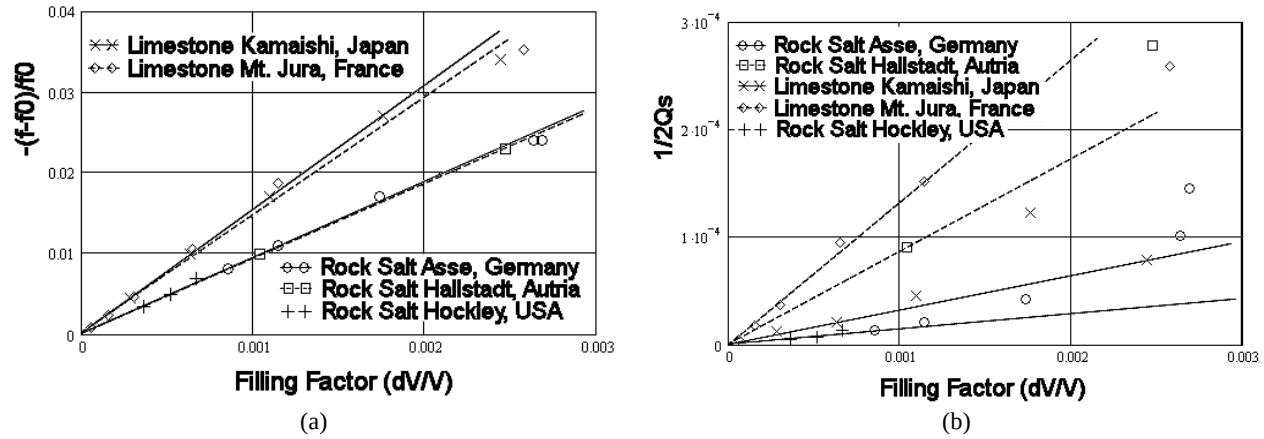

(a) (b)

Figure 6: Linearity of the perturbation measurements. (a) is the resonance frequency difference vs. filling factor for rock salt and lime stone samples. (b) is the inverse Q difference vs. filling factor for the rock salt and lime stone samples. If the perturbation formula holds, then a straight line should pass through all the data point cross the origin.

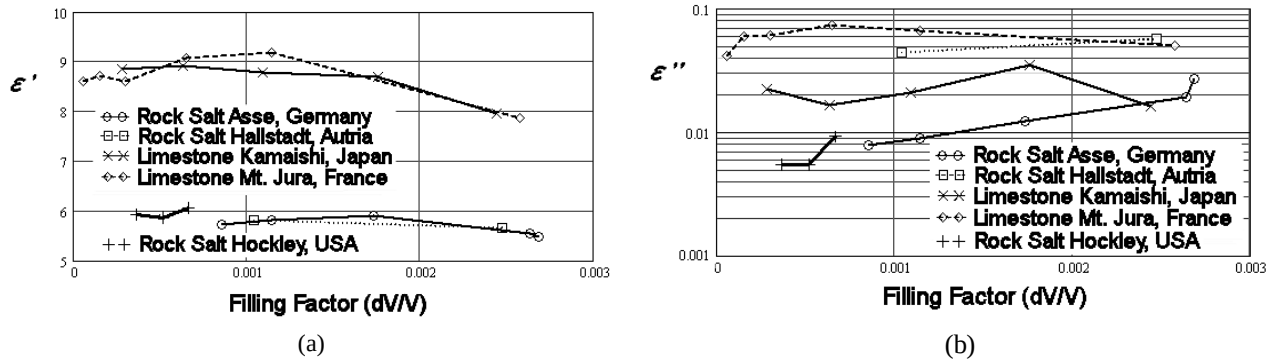

(a) (b)

Figure 7: Linearity of the perturbation measurements. (a) is the real part of the permittivity vs. filling factor for the rock salt and lime stone samples. (b) is the imaginary part of the permittivity vs. filling factor for the rock salt and lime stone samples. If the perturbation formula holds, then all the data points should be constant with respect to the filling factor.

The results of the measurements of ε' and ε'' are listed in Table 3. We find that for the real part of the permittivity ε', the size of the sample is sufficiently thin and the values for the Asse and Hallstadt samples at 5.8 ± 0.2 are consistent with the values for the synthetic rock salt. These values are also consistent with those obtained from the free space measurement, tabulated in Table 2.

For the imaginary part of the permittivity ε'', it seems that the samples were not sufficiently thin, in contrast to the synthetic rock salt samples. The results show that the thinner samples have smaller ε'' values. Therefore we are only able to estimate an upper limit for ε'', even for the smallest samples. We have calculated the attenuation coefficient α by Eq. (1). If there is no frequency dependence in $\tan\delta$, then since there is no orientational polarization in a material, i.e. ε''

is that same for all orientations, the attenuation lengths L_α calculated at 9.4 GHz, 7.7 m for the synthetic salt, can be extrapolated to other frequencies, e.g. at 94 MHz the attenuation length in a pure rock salt crystal is 770 m. Our results show that at lower frequencies, the attenuation length may be sufficiently long for use in a salt neutrino detector. Although there was a large uncertainty in ε'', we were able to obtain lower limits of the attenuation length.
In order to improve the accuracy of the measurements of ε'' we need thinner samples. Alternatively we could use a super conducting cavity resonator, which would have larger values of Q_0, e.g. 20000. In this case $1/Q_0$ in Eq. (11) becomes smaller and the uncertainty decreases.
If the perturbation formula holds, $-(f-f_0)/f_0$ and $1/Q_s$ are proportional to dV/V. As shown in Fig. 6(a), the linearity of $-(f-f_0)/f_0$ vs. dV/V holds up to a filling factor of about 1.7×10^{-3} for the Asse samples, 2.5×10^{-3} for the Hallstadt samples and 1.1×10^{-3} for the lime stone samples. For the Lime stone samples, the linearities are good below 1.1×10^{-3}. In addition, small stick samples below 1mm× 1mm are obtained for Jura lime stone. On the other hand, as shown in Fig. 6(b), the linearity of $1/Q_s$ do not hold for any of the rock salt samples, but do for the new Jura lime stone samples. These lime stone samples are rigid, so that we could cut them precisely by milling machine. Table 4 summarizes the findings of the analysis of the linearity.
Fig. 7 shows the dependence of ε' and ε'' on dV/V. If the linearity of the perturbation formula holds, the each component of the complex permittivity is constant.
The imaginary part of ε for the Jura lime stone was very large, 3 times larger than the Kamaishi lime stone. On the other hand, the Kamaishi lime stone had small loss, almost 2 times larger than the Asse rock salt.

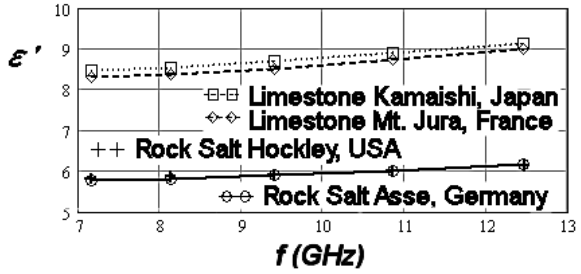

Figure 8(a): Frequency dependence of real part of the permittivity.

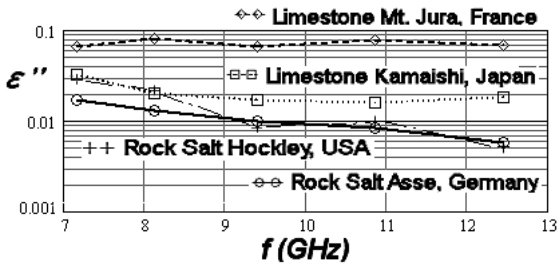

Figure 8(b): Frequency dependence of real part of the permittivity.

In order to get the data below 9.4GHz, we used another mode number of the cavity resonator. Fig. 8 is the frequency dependency of the complex permittivity of the three small stick samples, Jura lime stone, Kamaishi lime stone, Asse rock salt and Hockley rock salt The measurements were made at the frequency from 7GHz to 12GHz using $TE_{10,\ 3\text{-}9}$ mode cavity. The size of the samples are 1mm×1mm×10.2mm for Kamaishi lime stone and Jura lime stone, 1.4mm×1.3mm×10.2mm for Asse rock salt and 1.2mm×1.2 mm×10.2mm for Hockley rock salt. We selected the samples so that the linearity of the perturbation holds, but we could not obtain a small sample for Asse rock salt. As indicated in Fig. 8(a), the real part of ε is almost constant for all samples, but slightly increased at high frequencies. The linearity of the perturbation formula would not hold at higher frequencies. The measurement error at 7 GHz (n=3) is very large because the detected signals are very small and noisy. As shown in Fig. 8(b), the imaginary part of ε is constant for Jura lime stone sample, but increased at lower frequencies for Kamaishi lime stone, Asse rock salt and Hockley rock salt samples. At the present stage, the data are not fixed because the measurements were preliminary. Although the any measurement would difficult for low loss materials, further experiments below 7GHz are required.

5. DISCUSSION

Minimum sized SND is envisaged as shown in Fig. 1. Radio wave sensors of 216 are arrayed regularly in 200m repetitions inside a 1km×1km ×1km rock salt. The attenuation length becomes longer when we use the lower frequency to be detected. However the detection threshold energy of UHE neutrinos increases at the lower frequency. The optimization should be done to select the frequency. If the attenuation length is 400m, the sensor separation distance less than 200m is needed to detect the Cherenkov ring shape as well as the energy. Six radio sensors are hung on a string. The string is lowered in a well with the depth over 1km. At the total 36 wells should be bored.

There is a possibility to detect radio wave from the neutrino reaction as low as 1TeV if we could set the antennas nearby the shower[14]. According to the proposal for neutrino physics at LHC constructing at CERN[20], it could supply neutrinos over 1TeV from the collision points. The neutrinos are coming from charm and anti-charm quark decays since there is no π's and K's decay region. Then the beam would contain an equal number of ν_e's and ν_μ's unlike conventional beams. The beam would also contain an appreciable number of ν_τ's resulting from D_s decay. If we could use a space near the LHC tunnel e.g. the transfer line where it is located 500 m from the collision point 1, ATLAS experiment, it is enough to install smaller media e.g. rock salt or lime stone. It will become a good calibration test for the neutrino detection as well as the highest energy neutrino detection generated artificially. Due to their estimation, with the luminosity of $4x10^{34}cm^{-2}s^{-1}$, running time of 10^7s and the angular coverage of ±2.5mrad, a 15m long detector with a density of 7.86 gcm^{-3} and a total weight of 24 tons, 58,000 interactions are expected over 500GeV.
Lime stone is more common in the world than rock salt. Especially Japan has abundant in high purity lime stone. Unfortunately, lime stone tends to crack to be penetrated by water. Weak acid water melts lime stone and makes a lime stone cave. Therefore we could not expect a large amount of lime stone without including water. However we could expect a relatively small amount of the lime stone without water. Such a smaller size could be used to detect stronger neutrino beam emitted by LHC collision points. Mt. Jura is known to be made up of lime stone, which is situated within ~10km west from LHC collision point. The LHC ring located 100m underground. The north and the south collision points are used for CMS (point 5) and ATLAS (point 1) experiments, respectively.

6. CONCLUSION

Rock salt has been studied as a radio wave transmission medium in a UHE cosmic neutrino detector. The radio waves to be detected are those generated by the Askar'yan effect (coherent Cherenkov radiation from negative excess charges in an electromagnetic shower) for the interaction of UHE neutrinos in the rock salt. Samples from two rock salt mines were investigated to determine whether they are viable sites for an SND. They were the Asse mine in Germany, the Hallstadt mine in Austria and the Hockley salt mine. Furthermore, we took lime stone samples from a mine in Kamaishi, Japan and Mt. Jura, France.
The attenuation lengths of the samples were determined by the free space and the cavity perturbation methods. The attenuation lengths of radio wave at 9.4 GHz were found to be 7.7m, 4.7m, >3.3m, >0.56m, 1.9m and 0.5m for synthetic single crystals, the Hockley salt, the Asse rock salt, the Hallstadt rock salt, the Kamaishi lime stone and the Jura lime stone, respectively. A more definite estimate of the attenuation length will require thinner samples.
For rock salt, the radiation produced by the Askar'yan effect is strongest at about 6 GHz, at the Cherenkov angle of 66°, estimated by the density and the radiation length. At a frequency of 94 MHz the attenuation length is long enough to make a neutrino detector, although the radiation power is compromised and the threshold energy for the detection of neutrinos becomes higher. Recently, P. Gorham et al.[17] have measured attenuation length at the Waste Isolation Pilot Plant (WIPP), located in an evaporite salt bed in Carlsbad, New Mexico and found short attenuation lengths of 3-7m for frequencies of 150-300 MHz. On the contrary, measurements at United Salt's Hockley mine, located in a salt dome near Houston, Texas yielded attenuation lengths in excess of 250 m at similar frequencies. The measured value of the our attenuation lengths of the Hockley rock salt sample is 4.7m at 9.4 GHz and then under the assumption of constant $\tan\delta$ with respect to frequency, we estimate it by extrapolation to be longer than 290 m at 150 MHz. Their results are consistent with our estimated result for the Hockley sample.
The results of radio wave attenuation length in rock salt show that it is a possible medium for a UHE neutrino detector in a rock salt mine with a high transparency. We presented preliminary results of the complex permittivity with respect to frequency from 7 to 12 GHz, but the data were not fixed at the present stage. So we need to make perturbed cavity resonator measurements at lower frequencies and with more samples in order to make a concrete conclusion. Before the SND site is decided it is important to measure the attenuation length in situ as there may be defects and impurities in the salt at the site, as well as intrusions by minerals other than rock salt. For such a study the free space measurement method with transmission configuration as well as a ground-penetrating radar would be useful.
We have also made a study of a radiometer modified from a television broadcast satellite receiver, which showed a noise level of 150 K, a level low enough for use in an SND. It is a great advantage if we could use low cost receivers such as this because large numbers of antennas are required, spaced at less than 200m in a 1km×1km×1km mass of rock salt. The attenuation in the rock salt and the radiation pattern of coherent Cherenkov radiation require that the antennas are repeated in such a way. The frequency to be detected should be decided upon after taking into account the detection energy threshold of the UHE neutrinos and the attenuation length at that frequency. In addition, in order to calibrate the

energy of the initial electromagnetic shower produced in the interaction of the neutrinos with the rock salt and the distribution of radiation power, which depends on the degree of coherency, an important study is that of the basic processes of coherent Cherenkov radiation due to a pulsed electron and a neutrino beam by supplied in an accelerator[32].

7. ACKNOWLEDGMENT

This work was supported partly by Funds for Special Research Project at Tokyo Metropolitan University, Fiscal Year 1999 and Agilent Technologies University Relations Philanthropy Grants Program Fiscal Year 2001.This work is also partially supported by a Grant in Aid for Scientific Research from Ministry of Education, Science, Sports and Culture of Japan in Fiscal Year 2002. We wish to express our appreciation to Ms. M. Kawaki, Ms. M. Ikeda, Dr. H. Athar and Dr. O.Yasuda for their involvement and support of this project. For getting Jura lime stone sample, cooperation with Prof. M. Kobayashi (KEK) was done. We express our gratitude to M.E. Ryoichi Ueno who discussed with us and advised us on the microwave techniques. His help was indispensable in carrying out this study.
The research could not be possible without the assistance of many different people who I could not list in this paper[10, 22].

8. REFERENCES

1. F. W. Stecker, C. Done, M. H. Salamon and P. Sommers, "*High-Energy Neutrinos from Active Galactic Nuclei*", Phys. Rev. Lett. **66**, pp.2697-2700, 1991.
2. S. Barwick, F. Halzen, D. Lowder, T. Miller, Morse, P.B. Price and A. Westphal, "*Neutrino astronomy on the 1km^2 scale*", J. Phys. G: Nucl. Part. Phys. **18**, pp.225-247, 1992; Thomas K.Gaisser, Francis Halzen, Todor Stanev, "*Particle astrophysics with high energy neutrinos*", Phys. Reports **258**, pp173-236, 1995; Alvarez-Muniz and F. Halzen, "*10^{20}eV cosmic-ray and particle physics with kilometer-scale neutrino telescopes*", Phys. Rev. **D63**, pp.037302-1, 037302-4, 2001.
3. Takeda et al., "*Extension of the Cosmic-Ray Energy Spectrum beyond the Predicted Greisen-Zatsepin-Kuz'min Cutoff*", Phys. Rev. Lett. **81**, pp.1163-1166, 1998.
4. K. Greisen, "*End to the Cosmic-Ray Spectrum?*" Phys. Rev. Lett. **16**, p.748, 1966; G.T. Zatsepin, V.A. Kuz'min, Zh. Eksp. Teor. Fiz., Pis' ma Red. **4**, p.114, 1966 [Soviet Physics JETP Lett. **4**, p.78, 1966].
5. G. Burdman, F. Halzen and R. Gandhi, "*The highest energy cosmic rays and new particle physics*", Phys. Lett. **B417**, pp.107-113, 1997; P. Jain, D.W. Mckay, S. Panda, J. P. Ralston, "*Extra dimensions and strong neutrino-neutrino-nucleon interactions above 10^{19}eV: breaking the GZK barrier*", Phys. Lett. **B484**, pp.267-274, 2000.
6. R. Gandhi, C. Quigg, M.H. Reno and I. Sarcevic, "*Ultrahigh-energy neutrino interactions*", Astroparticle Phys. **5**, pp.81-110, 1996; "*Netrino interactions at ultrahigh energies*", Phys. Rev. **D58**, 093009; Sigl, G. Phys. Rev. **D57**, pp.3786-3789, 1998; J. Kwiecinski, A.D. Martin, A.M. Stasto, "*Penetration of the Earth by ultrahigh energy neutrinos predicted by low x QCD*", Phys. Rev. **D59**, 093002, 1999; R. Horvat, "*Propagation of ultrahigh-energy neutrinos through the earth*", Phys. Lett. **B480**, pp.135-139, 2000.
7. J.G. Lerarned and S. Pakvasa, Astropart. Phys. **3**, p.267, 1995; F. Halzen and D. Saltzberg, "*Tau Neutrino Appearance with a 1000 Megaparsec Baseline*", Phys. Rev.Lett. **81**, pp.4305-4308, 1998 ; H. Athar, M. Jezabek and O. Yasuda, "*Effects of neutrino mixing on high-energy cosmic neutrino flux*", Phys. Rev. **D62**, pp.103007-1, 103007-8, 2000; H. Athar, "*Tau neutrinos from active galactic nuclei*", Nucl. Phys. B (Proc. Suppl.) **76**, p.419, 1999; H. Athar, G. Parente and E. Zas, "*Prospects for observations of high-energy cosmic tau neutrinos*", Phys. Rev. **D62**, 093010-1, 093010-5, 2000.
8. M. Chiba, T. Kamijo, M. Kawaki, H. Athar, M. Inuzuka, M. Ikeda, O. Yasuda, "*Study of Salt Neutrino Detector*", Proc. 1st International Workshop for Radio Detection of High Energy Particles [RADHEP-2000], UCLA, AIP Conference Proceedings, Vol. **579**, pp.204-221, November 16-18, 2000.; T. Kamijo and M. Chiba, "*A Microwave Properties of Rock Salt and Lime stone for an Ultra-High Energy Neutrino Detector"*, Memoirs of Faculty of Tech., Tokyo Metropolitan University, No.**51 2001**, pp.139-156 (2002) ;M. Chiba et. al., "*Measurement of Attenuation Length in Rock Salt and Lime stone in Radio Wave for Ultra-High Energy Neutrino Detector*", Presented at the First NCTS (National Center for Theoretical Sciences) Workshop on Astroparticle Physics, Dec.6-Dec.9, 2001, Taiwan. The proceeding will be published World Scientific Publishing Co. Ltd.

9. T. Machida et al (ed.), *"Topography dictionary"* (in Japanese) , Ninomiya Book Co. Ltd., Tokyo, pp.110, 1981; J. L. Stanley, "*Handbook of World Salt Resources*", Plenum Press, New York, 1969; T. H. Michel, "*Salt Domes*", Gulf Publishing Company, Houston, 1979.
10. Y. Fukuda et al., SuperK Collaboration, "*Evidence for Oscillation of Atmospheric Neutrinos*", Phys. Rev. Lett. **81**, p.1562, 1998.
11. National Astronomical Observatory of Japan (ed.), "*Chronological Scientific tables*" (in Japanese), Maruzen Co. Ltd., Tokyo, p.486, 1998.
12. P. Gorham, D. Saltzberg, A. Odian, D. Williams, D. Besson, G.Fichter and S. Tantawi, "*Measurements of the Suitability of Large Rock Salt Formations for Radio Detection of High Energy Neutrinos*", hep-ex/0108027 v1 **14,** Aug 2001.
13. J.C. Cook, "*Radar Transparencies of Mine and Tunnel Rocks*", Geophysics **40**, pp.865-885, 1975.; E. Mundry, R. Thierbach, F. Sender and H. Weichart, "*Borehole Radar Probing in Salt Deposits*", Proceedings of the Sixth International Symposium on Salt, **Vol.I**, pp.585-599, 1983; H. Nickel, F. Sender, R. Thierbach and H. Weichart, "*Exploring the Interior of Salt Domes from Boreholes*", Geophysical Prospecting **31**, pp.131-148, 1983; M. Sato and R. Thierbach, "*Analysis of a Borehole Radar in Cross-Hole Mode*", IEEE Trans. on Geoscience and Remote Sensing, **29**, pp.899-904, 1991; D. Eisenburger, "*Evaluation and Three-Dimensional Representation of Ground-Probing Radar Measurements*", Proceedings of the 5th International Conference on Ground Penetrating Radar, pp.647-659, 1994; D. Eisenburger, V. Gundelach, F. Sender, R. Thierbach, "*Underground Radar Studies for Solving Geological and Safeguarding Problems in Nuclear Waste Repositories*", Proceedings of the 6th International Conference on Ground Penetrating Radar, pp.427-432, 1996.
14. F. Halzen, E. Zas, T. Stanev, "*Radio detection of cosmic neutrinos. A numerical, real time analysis*", Phys. Lett. **B257**, pp.432-436, 1991; E. Zas, F. Halzen, T. Stanev, "*Electromagnetic pulses from high-energy showers: Implications for neutrino detection*", Phys. Rev. **D45**, pp.362-376, 1992; J. Alvarez-Muniz and E. Zas, "*Cherenkov radio pulses from EeV neutrino interactions: the LPM effect*", Phys. Lett. **B411**, pp.218-224, 1997; G.M. Frichter, J.P. Ralston and D.W. Mckay, "*On radio detection of ultrahigh energy neutrinos in Antarctic ice*", Phys. Rev. **D53**, pp.1684-1698, 1996.; M.A. Markov and IM Zheleznykh, "*Large-Scale Cherenkov Detectors in Ocean, Atmosphere and Ice*", Nucl. Instrum. Methods. **A248**, pp.242-251, 1986.
15. G.A. Askar'yan, "*Excess Negative Charge of an Electron-Photon Shower and its Coherent Radio Emission*", Zh. Eksp. Teor. Fiz. **41**, pp.616-618, 1961 [Soviet Physics JETP **14**, pp.441-442 (1962)]; G.A. Askar'yan, "*Coherent Radio Emission from Cosmic Showers in Air and in Dense Media*", Soviet Physics JETP **48**, pp.988-990, 1965 [**21**, pp.658 – 659, 1965].
16. M. Fujii and J. Nishimura, "*Radio wave emission from extensive air showers*", Proc. 11th Int. Conf. On Cosmic Rays, Butapest, pp.709-715, 1969.
17. P. Gorham, D. Saltzberg, , P.Schoessow, W. Gai, J. G. Power, R. Konecny and M.E. Conde, "*Radio-frequency Measurements of Coherent Transition and Cherenkov Radiation: Implication for High-energy Neutrino Detection* ", Phys. Rev. **E62**, pp.8590-8605, 2000. ; D. Saltzberg, P. Gorham, D. Walz et al., "*Observation of the Askaryan Effect: Coherent Microwave Cherenkov Emission from Charge Asymmetry in High-Energy Particle Cascades*", Phys. Rev. Lett. **86**, p.2802, 2001.
18. R. Ueno, T. Kamijo, K. Hatakeyama and N. Ogasawara, "*The Measurement of Scattering Coefficients of Radio-Wave Scatter-Suppressors at the Microwave Region*"(in Japanese), Record of Study, I.E.C.E., Japan, **CPM 77-106**, pp.99-102, 1978.; R. Ueno and N. Ogasawara, "*On the Measurement of Scattering Coefficient of Radio-Wave Scatter Suppressor*", Memoirs of Faculty of Technology, Tokyo Metropolitan University, No.**30 1980**, pp.2907-2916, 1981.; R. Ueno and T. Kamijo, "*A Method for the Measurement of Scattering Coefficients at the Microwave Region*", Memoirs of Faculty of Tech., Tokyo Metropolitan University, No.**48 1998**, pp.5743-5752 (1999); R. Ueno and T. Kamijo, "*Method for the Measurement of Scattering Coefficients Using a Metal-Plate Reflector in the Microwave Region*", IEICE Trans. Commun. **E83B**, pp.1554-1562, 2000.
19. R. Ueno and T. Kamijo, "*The Measurement of Complex Permittivity Using a Simply Designed Perturbed Cavity Resonator at Microwave Frequencies*", Memoirs of Faculty of Technology, Tokyo Metropolitan University, No.**38 1988**, pp.3923-3933 (1989)
20. L. Camilleri, "*Neutrino Physics at LHC*", Large Hadron Collider Workshop, held at Aachen, 4-9 October 1990, Proceedings Vol. III (G. Jalskog and D. Rein Ed.), CERN 90-10 ECFA 90-133, Volume **III 3**, December 1990.